Cortical Num1p Interacts with the Dynein Intermediate Chain Pac11p and Cytoplasmic Microtubules in Budding Yeast

Marian Farkasovsky and Hans Küntzel

Max-Planck Institute for Experimental Medicine, D-37075 Göttingen, Germany

Abstract. Num1p, a cortical 313-kD protein, controls cytoplasmic microtubule (cMT) functions and nuclear migration through the bud neck in anaphase cells. A green fluorescent protein (GFP)-Num1p fusion protein localizes at the bud tip and the distal mother pole of living cells, apparently forming cMT capture sites at late anaphase. In addition, galactose-induced GFP-Num1p is seen at the bud neck and in lateral regions of the mother cortex. The bud tip location of Num1p depends on Bni1p but does not require Kar9p, Dyn1p, or cMTs, whereas cMT contacts with polar Num1p dots are reduced in cells lacking Dyn1p. Num1p associates with the dynein intermediate chain Pac11p in the presence of Dyn1p, and with the α-tubulin Tub3p, as shown by coimmune precipitation of tagged proteins. Num1p also forms a complex with Bni1p and Kar9p, although Num1p is not required for Bni1p- and Kar9p-dependent nuclear migration to the bud neck in preanaphase cells.

Our data suggest that Num1p controls nuclear migration during late anaphase by forming dynein-interacting cortical cMT capture sites at both cellular poles. In addition, Num1p may transiently cooperate with an associated Bni1p–Kar9p complex at the bud tip of early anaphase cells.

Key words: microtubule • cytoskeleton • nuclear migration • dynein • yeast

Introduction

Two subsequent steps of nuclear migration are required for chromosome segregation in the budding yeast *Saccharomyces cerevisiae*: the proper positioning of the short preanaphase spindle at the mother bud neck, followed by the movement of the elongating spindle and nucleus through the neck during anaphase. Both nuclear migration steps depend on the functions of kinesin-related motor proteins and are controlled by physical interactions between the plus-ends of cytoplasmic microtubules (cMTs)[1] and cortical proteins serving as cMT capture sites (Yeh et al., 1995; Carminati and Stearns, 1997; DeZwaan et al., 1997; Shaw et al., 1997, 1998; Kahana et al., 1998; Cottingham and Hoyt, 1997; Adames and Cooper, 2000; Heil-Chapdelaine et al., 2000; Hildebrandt and Hoyt, 2000).

The first step, nuclear migration to the bud neck and alignment of the short spindle along the mother–daughter axis in preanaphase cells, requires the interaction of the plus-ends of bud-oriented cMTs with the cortical protein Kar9p (Miller and Rose, 1998). The Kar9p localization at the bud tip cortex depends on its interaction with the formin Bni1p, the actin-interacting protein Bud6p/Aip3p, and F-actin (Lee et al., 1999; Miller et al., 1999; Theesfeld et al., 1999; Lee et al., 2000). Furthermore, the cMT capture by cortical Kar9p requires Bim1p/Yeb1p, a protein of the EB1 family localized at the plus-ends of microtubules (Schwartz et al., 1997; Tirnauer et al., 1999; Adames and Cooper, 2000; Korinek et al., 2000; Lee et al., 2000; Miller et al., 2000), and the kinesin-related motor protein Kip3p (Cottingham and Hoyt, 1997; DeZwaan et al., 1997).

The movement of the elongating spindle through the bud neck during anaphase (the second step of nuclear migration) involves dynein (Dyn1p), a minus-end–directed microtubule motor, its actin-binding regulator dynactin (Act5p/Arp1p, Nip100p, Jnm1p), and the kinesin-related motor Kip2p (Saunders et al., 1995; Yeh et al., 1995; Carminati and Stearns, 1997; Shaw et al., 1997, 1998; Kahana et al., 1998; Miller et al., 1998; Adames and Cooper, 2000). Filamentous actin is not required for the dynein-dependent spindle movement through the neck (Heil-Chapdelaine et al., 2000).

Cortical proteins interacting with the dynein–dynactin complex at cMT capture sites have been postulated (Carminati and Stearns, 1997; Heald and Walczak, 1999; Karki and Holzbaur, 1999; Hildebrandt and Hoyt, 2000) but remain to be identified. A possible candidate is Num1p, a large protein (313 kD), which was localized by indirect immunofluores-

Address correspondence to Hans Küntzel, Max-Planck-Institut für Experimentelle Medizin, Hermann-Rein-Strasse 3, D-37075 Göttingen, Germany. Tel.: 49-0551-3899-278. Fax: 49-0551-3899-352. E-mail: kuentzel@em.mpg.de

Marian Farkasovsky's present address is Slovak Academy of Sciences, Institute of Molecular Biology, 84251 Bratislava, Slovakia.

[1]*Abbreviations used in this paper:* cMT, cytoplasmic microtubule; GFP, green fluorescent protein; HA, hemagglutinin; Myc, c-Myc; PH, pleckstrin homology; SPB, spindle pole body; yEGFP, yeast-enhanced GFP; YPD, yeast extract/peptone plus dextrose.

Table I. Yeast Strains

Strain	Genotype
FY1679 background	
FY1679	*MATa/MATα ura3-52/ura3-52 leu2-Δ1/LEU2 trp1-Δ63/TRP1 his3-Δ200/HIS3*
FMY691	*a ura3 leu2 trp1 his3*
FMY693	*a ura3 trp1 his3 num1Δ::loxP*
FMY711	*a ura3 bni1Δ::kanMX4*
FMY705	*a ura3 leu2 his3 kar9Δ::kanMX4*
FMY859	*a ura3 leu2 trp1 his3 dyn1Δ::kanMX4*
FMY856	*a ura3 leu2 trp1 his3 arp1Δ::TRP1*
FMY848	*a ura3 kip2Δ::kanMX4*
FMY852	*a ura3 kip3Δ::kanMX4*
FMY821	*a ura3 leu2 trp1 his3 num1Δ::loxP bni1Δ::TRP1*
FMY799	*a ura3 leu2 trp1 his3 num1Δ::loxP kar9Δ::TRP1*
FMY789	*a ura3 leu2 trp1 his3 num1Δ::HIS3MX6 dyn1Δ::TRP1*
FMY793	*a ura3 leu2 trp1 his3 num1Δ::loxP arp1Δ::TRP1*
FMY850	*a ura3 leu2 trp1 his3 num1Δ::loxP kip2Δ::kanMX4*
FMY854	*a ura3 leu2 trp1 his3 num1Δ::loxP kip3Δ::kanMX4*
FMY519	*a/α ura3/ura3 leu2/+ trp1/+ his3/+ num1::kanMX4-GAL1p-yEGFP3-NUM1/NUM1*
FMY627	*a ura3 leu2 num1::kanMX4-GAL1p-yEGFP3-NUM1*
FMY795	*a/αura3/ura3 leu2/leu2 bni1Δ::kanMX4/bni1Δ::kanMX4 num1::loxP-GAL1p-yEGFP-NUM1/NUM1*
FMY838	*a/αura3/ura3 leu2/leu2 trp1/+ his3/his3 kar9Δ::kanMX4/kar9Δ::kanMX4 num1::loxP-GAL1p-yEGFP3-NUM1/NUM1*
FMY872	*a/αura3/ura3 leu2/+ trp1/+ dyn1Δ::kanMX4/dyn1Δ::kanMX4 num1::loxP-GAL1p-yEGFP-NUM1/NUM1*
CEN.PK2 background	
CEN.PK2	*MATa/MATα ura3-52/ura3-52 leu2-2,112/leu2-3,112 trp1-289/trp1-289 his3-Δ1/his3-Δ1*
FMY684	*a/αnum1::kanMX4-GAL1p-3xMyc-NUM1/NUM1*
FMY899	*a/αpac11::kanMX4-GAL1p-3xHA-PAC11/PAC11*
FMY682	*a/αtub3::kanMX4-GAL1p-3xHA-TUB3/TUB3*
FMY783	*a/abni1::kanMX4-GAL1p-3xHA-BNI1/BNI1*
FMY810	*a/αkar9::kanMX4-GAL1p-3xHA-KAR9/KAR9*
FMY905	*a/αnum1::kanMX4-GAL1p-3xMyc-NUM1/NUM1*
FMY912	*a/αnum1::kanMX4-GAL1p-3xMyc-NUM1/NUM1 pac11::kanMX4-GAL1p-3xHA-PAC11/PAC11 dyn1Δ::HIS3/dyn1Δ::HIS3*
FMY603	*a/αnum1::kanMX4-GAL1p-3xMyc-NUM1/NUM1 tub3::kanMX4-GAL1p-3xHA-TUB3/TUB3*
FMY805	*a/αnum1::kanMX4-GAL1p-NUM1/NUM1 bni1::kanMX4-GAL1p-3xHA-BNI1/BNI1*
FMY809	*a/αnum1::kanMX4-GAL1p-3xMyc-NUM1/NUM1 kar9::kanMX4-GAL1p-3xHA-KAR9/KAR9*
FMY861	*a/αnum1::kanMX4-GAL1p-YEGFP3-NUM1/NUM1 kar9::kanMX4-GAL1p-3xHA-KAR9/KAR9*

cence microscopy mainly to the mother cortex of budded cells (Kormanec et al., 1991; Farkasovsky and Küntzel, 1995). The cortical association and nuclear migration control functions of Num1p were shown to depend on a COOH-terminal pleckstrin homology (PH) domain (Farkasovsky and Küntzel, 1995). The deletion of *NUM1* does not affect viability but causes the accumulation of large-budded cells with two DAPI-stained chromosomal regions in the mother compartment, especially after entering the stationary phase (Kormanec et al., 1991; Revardel and Aigle, 1993). *num1*Δ strains are synthetic lethal with certain cold-sensitive *tub2* alleles and contain abnormally long and mislocated cMTs (Farkasovsky and Küntzel, 1995), as observed in *dyn1*Δ and *arp1*Δ mutants (Muhua et al., 1994; Carminati and Stearns, 1997).

A synthetic lethality screen with a strain deficient in the kinesin-related motor protein Cin8p has identified Num1p/Pac12p, together with 19 other gene products, as a protein required for viability in the absence of Cin8p (Geiser et al., 1997). Mutant alleles of eight *PAC* (perish in the absence of Cin8p) genes, including *NUM1*, caused phenotypes similar to *dyn1*Δ and *arp1*Δ strains, including a spindle-positioning defect, suggesting that Num1p acts in a dynein–dynactin pathway (Geiser et al., 1997). Furthermore, Num1p shares with Dyn1p the property that it is required for viability in the absence of the cMT-binding protein Bim1p (Schwartz et al., 1997).

Here, we report the localization of a green fluorescent protein (GFP)-Num1p fusion protein (controlled by its own promoter) at the bud tip and the distal pole of the mother cortex in living cells. Additional GFP-Num1p dots are seen at the bud neck and the mother cortex upon fusion to the *GAL1* promoter and galactose-induced overproduction. The Num1p patches at both cellular poles are often intersected by cMTs at late anaphase/telophase, and the dynein heavy chain Dyn1p appears to be important to mediate Num1p–cMTs contacts.

We further demonstrate that Num1p forms a complex with the dynein intermediate chain Pac11p, if Dyn1p is present, and with the α-tubulin Tub3p, suggesting a dynein-anchoring function of Num1p at cMT capture sites. In addition, we present evidence that Num1p coexists and associates with Bni1p and Kar9p at the bud tip of early anaphase cells, although Num1p is not required for Bni1p- and Kar9p-dependent nuclear migration to the bud neck in preanaphase cells.

Materials and Methods

Strains, Media, and Genetic Techniques

Genotypes of the yeast strains used in this study are listed in Table I. Media, genetic techniques, and the lithium acetate method of yeast transformation were as described (Ausubel et al., 1993). PCR-based gene deletions and modifications were carried out as described (Longtine et al., 1998), using plasmids pFM224 and pFM225 (Ansari et al., 1999). Table II summarizes the codes and sequences of primers: S1 and S2 were used for gene deletions, N1 and N2 for NH_2-terminal protein tagging, and A1 for verification of correct insertion/replacement. *Taq* DNA polymerase (Expand™ High Fidelity PCR System) was purchased from Roche Molecular Biochemicals. Plasmid pFM206 contains a *kanMX4-GAL1p-yEGFP3* cassette and was constructed as follows: the *GAL1* promoter was inserted as a 0.8-kb EcoRV/SpeI fragment of pFM110 (*GAL1p* in pBluescript II KS) between the respective sites of pUG6 (Güldener et al., 1996). A 0.7-kb BamHI/SpeI PCR fragment containing *yEGFP3* (Cormack et al., 1997) was inserted between the respective sites of pUG6-*GAL1p* to obtain pFM204. A linker encoding the decapeptide GPDGAPADGP was inserted between the SpeI and SacII

Table II. Primers Used for PCR

Name	Sequence (5′–3′)*
NUM1-A1	GCT GAT AGA CCA AGT GTG GAT C
NUM1-S1	GCC AGG AAA GCG TCT CAA CGA ACG GCG TAA CAA GGA TGG CGC TGA AGC TTC GTA CGC TGC AGG
NUM1-S2	GCC AAA TGA TCG GCT TTG TGG TAC TCT ATG TCT TAG AGA CCC GCA TAG GCC ACT AGT GGA TCT G
NUM1-N1	GCT TTA GGA ACC ATA GAT TCC TGC GTA ATT TGT GGC CGC TTT ATT GGG CTG AAG CTT CGT ACG CTG CAG G
NUM1-N2	GCT GTC TTT ATC GTT ATT CTT TTT ATG CCT GTT GTT GTG GGA CAT TGG ACC ATC AGC TGG AGC ACC
KAR9-A1	GAT GGA TCA GTG GTA GAA ATG G
KAR9-S1	GCA CTG CCA TGG ATA ATG ATG GAC CCA GAT CTA TGA CCA TTG GGG ATG GCT GAA GCT TCG TAC GCT GCA GG
KAR9-S2	GGA GGC CTC AAT CGG GTT CTT CTT CTT GTC GAA GGG ACC CAA ACC GCA TAG GCC ACT AGT GGA TCT G
KAR9-N1	GGA TTT TCA TTA CCC GAA TCG ATA CTT TTG GTA GCA TAA ACA AAT AGC TGA AGC TTC GTA CGC TGC AGG
KAR9-N2	GGA AGT CAT CCC CAA TGG TCA TAG ATC TGG GTC CAT CAT TAT CCA TTG GAC CAT CAG CTG GAG CAC C
BNI1-A1	GGA GTT GGT ATG GAT AGA GC
BNI1-S1	CGA ACT CAA AGG AAA GTC ATT CGA ATT CGA GTT CTG GTA TAT TCC GCT GAA GCT TCG TAC GCT GCA GG
BNI1-S2	GCT CTG TCA CTA ATT TCC TCT TGA TCT TCC AGC GCA GAT GTC CGC ATA GGC CAC TAG TGG ATC TG
BNI1-N1	GCA CGG ACC CTT CCT ACA GAT AAG AGG ACA CTG ACG GCT GTG TGT TAG CTG AAG CTT CGT ACG CTG CAG G
BNI1-N2	GAC TTT CCT TTG AGT TCG AAT GTT TGG AGC CTG AAT TCT TCA ACA TTG GAC CAT CAG CTG GAG CAC C
DYN1-A1	GGT GTG TCT ATC CGT TCT AAC
DYN1-S1	GGC AGA AAC CAT TAA GAG TAT ATC CCC TTC TAC TTA TCA CGA AGG CTG AAG CTT CGT ACG CTG CAG G
DYN1-S2	CCA TCT CTC CAC TCT AGC GTT GCT TTA AGC ATA CTT CCA TAC AAG GCG CAT AGG CCA CTA GTG G
ARP1-A1	GGA CAC AGT ACA CCT GTG TGA CG
ARP1-S1	GCC AAT GGA CCA GCT AAG TGA CAG CTA TGC TTT GTA CAA TCA ACC CGT ACG CTG CAG GTC GAC
ARP1-S2	GCG TTG TAG TTC CGC CAC TTA GGA TTA TCG ATG ACA GTA AAG GAT CGA TGA ATT CGA GCT CG
KIP2-A1	CCA TTG TTC TAT GCT GCT GC
KIP2-S1	CCA AGC TTA AGG AGG CCA TCA ACG AGG TCT AGT TCT GGT TCA AGT GCT GAA GCT TCG TAC GCT GCA GG
KIP2-S2	CGT TAT CCA CGA CAG GGT GCG GTG ATT GCT GTG TAT TAA TGA GTG CGC ATA GGC CAC TAG TGG ATC TG
KIP3-A1	CCT TGT TTG ATG ACT TTA GTA TGG
KIP3-S1	CCA GCT GTA TAC TAT TGA CAC TAA CAT GAA CGT GCC TGA AAC AAG GCT GAA GCT TCG TAC GCT GCA GG
KIP3-S2	GGA AAG AAG TTA TAT TCG ATA GTT TAC GTA GGA TAT GTA TGT TAC GCA TAG GCC ACT AGT GGA TCT G
TUB3-A1	CCA ACT CGT TAC AGA TCT ACT GC
TUB3-N1	CAA ACC CCT TAC ATA ATC TAT AAA TAC TGT CAG GTT ACA TAT GCT GAA GCT TCG TAC GCT GCA GG
TUB3-N2	GGA ACG CAT ACA TAC CAT TAA TAC TAA TGA CCT CTC TCA TTG GAC CAT CAG CTG GAG CAC C
EGFP-As-T1	TTC GAA ATG TCT AAA GGT GAA GAA TTA TTC ACT GG
EGFP-As-T2	CCT CGA TTC GAA CCC TCG AGT TTG TAC AAT TCA TCC ATA CCA TGG
EGFP-Ba-T1	GCA TGG ATC CAT GTC TAA AGG TGA AGA ATT ATT CAC TGG
EGFP-Sp-T2	GGT CAA CTA GTT GGT TTG TAC AAT TCA TCC ATA CCA TGG

*Underlined sequences are portions of the corresponding genes.

sites of pFM204 to obtain pFM206. Insertion of the pFM206-derived PCR cassette at the *NUM1* translational start leads to the galactose-inducible expression of a highly fluorescing yeast-enhanced GFP (yEGFP)-Num1p fusion protein. Plasmid pFM313 contains a NH_2-terminal *yEGFP-NUM1* fusion under the control of the *NUM1* promoter in pRS416 (*CEN6/ARSH4/URA3*). A 0.7-kb BstBI PCR fragment (*EGFP*-As-T1 and *EGFP*-As-T2 primers) containing *yEGFP3* (Cormack et al., 1997) was inserted into the BstBI site of pJK23 located at the *NUM1* translational start (Kormanec et al., 1991). Further construction steps were used as described for pFM18 (Farkasovsky and Küntzel, 1995).

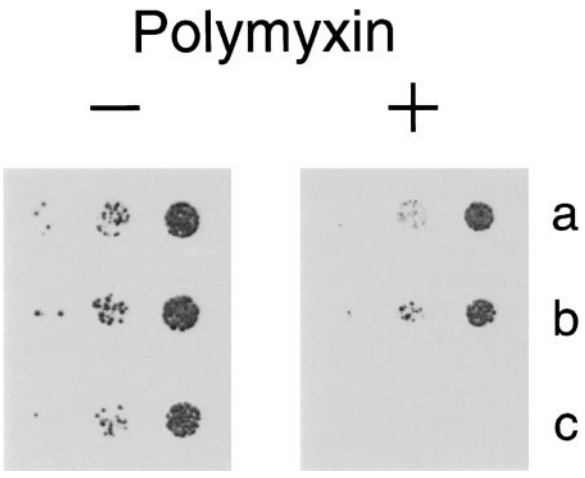

Figure 1. Polymyxin B sensitivity of *num1*Δ and *yEGFP3-NUM1* strains. Suspensions containing 10, 100, or 1,000 cells (from left to right) of haploid strains FMY691 (a, *NUM1*), FMY627 (b, *yEGFP3-NUM1*) and FMY693 (c, *num1*Δ) were dotted onto YPGal solid media without (left) or with (right) 0.3 mg/ml polymyxin B.

Immunological Methods

Strains expressing epitope-tagged proteins were grown in yeast extract/peptone plus dextrose (YPD) at 30°C to A_{600} = 0.3. Cells were collected by centrifugation, washed twice with YPGal (1% yeast extract, 2% peptone, 2% galactose), resuspended in YPGal, and grown for 4 h at 30°C. Protein extract preparation, immunoprecipitation, and Western blot analysis was performed as previously described (Ansari et al., 1999), with the following modification: the pelleted protein A–conjugated sepharose beads containing the immunocomplex were washed two times with IP buffer containing 0.1% Triton X-100 and 0.1% Tween 20, two times with IP buffer containing 0.1% Triton X-100, 0.1% Tween 20 and 100 mM NaCl, and one time with IP buffer. Beads were incubated in wash steps with 700 μl for 20 min at 4°C under constant agitation.

Fluorescence Microscopy

Overnight cultures of strains producing yEGFP-Num1p were diluted to A_{600} = 0.1 and grown in YPD to early log phase. Cells were collected by centrifugation, washed, and resuspended in YPGal with 0.3% glucose. After 2–3 h induction at 30°C (A_{600} = 0.6–0.8), living or fixed cells were immobilized with 2% agarose in PBS or minimal media. To preserve yEGFP fluorescence and to visualize microtubules or DNA, cells were fixed with formaldehyde added to a final concentration of 4% and incubated at room temperature for 90 min. Cells were then treated with monoclonal anti–α-tubulin or with DAPI (Sigma-Aldrich), as described previously (Farkasovsky and Küntzel, 1995). For nocodazole treatment, a strain containing the yEGFP-

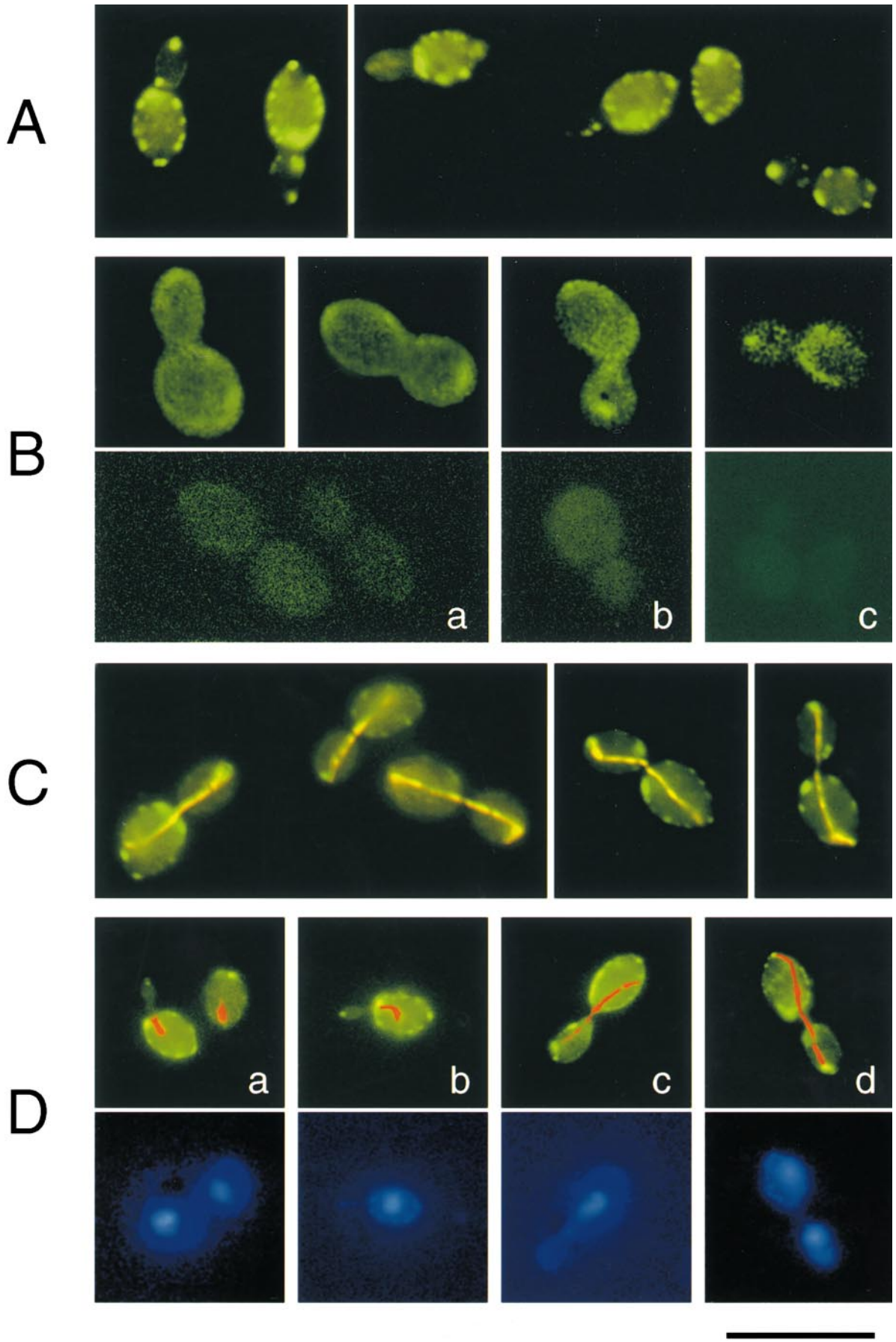

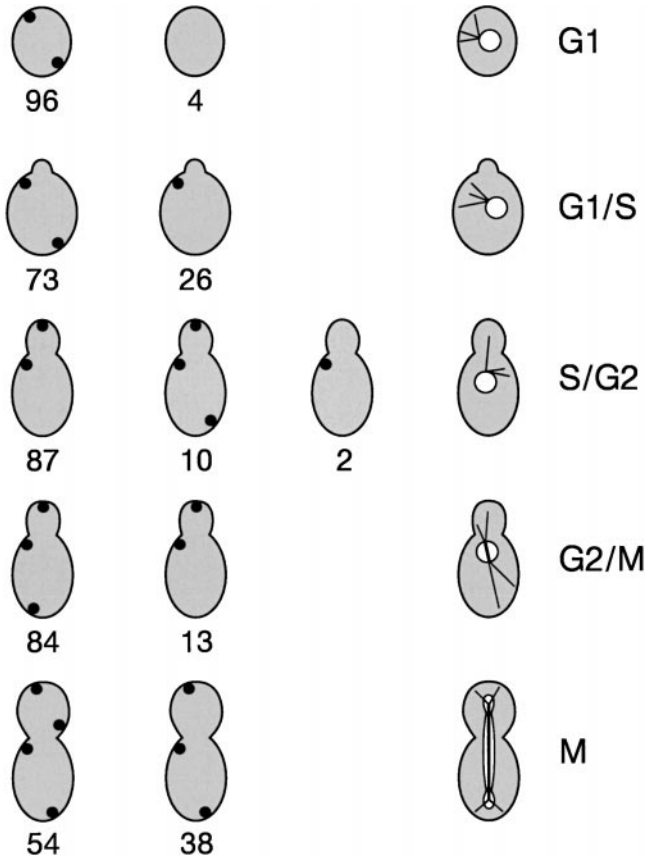

Figure 3. Quantification of cell cycle–dependent localization of galactose-induced GFP-Num1p. 200–250 cells (FMY519) of different stages, as determined by nuclear and microtubule positions, were scored for prominent cortical dot positions at cellular poles and bud neck sites. Additional dots at the mother cortex are not depicted.

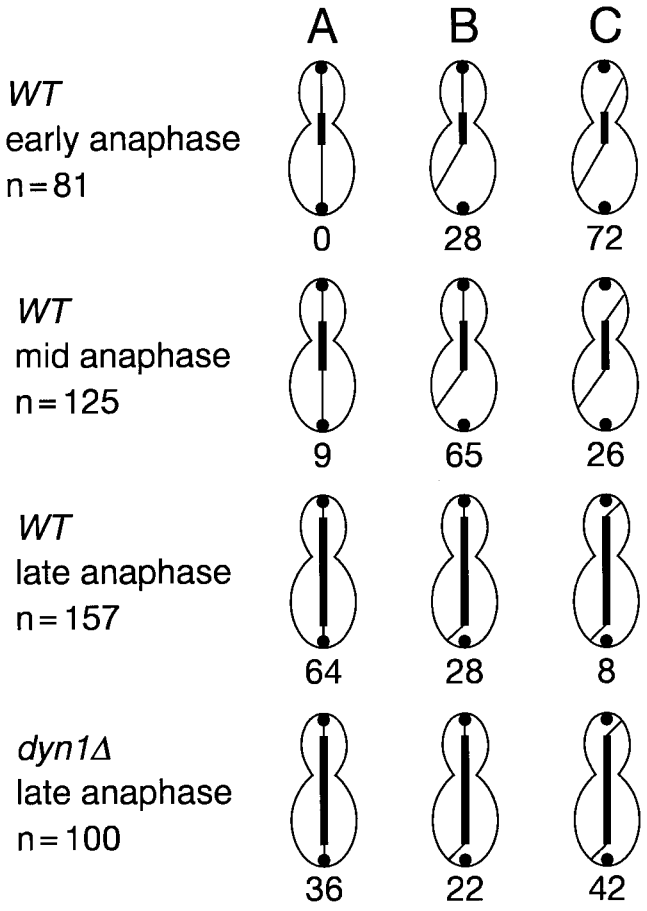

Figure 4. Quantification of cMT–cortex interactions in *WT* (FMY519) and *dyn1*Δ (FMY872) anaphase cells expressing galactose-induced GFP-Num1p. The percentage of cells with indicated cMT–cortex contacts was determined for early anaphase cells (short spindle entering the bud), mid anaphase cells (partially elongated spindle spanning the neck), and late anaphase cells (fully elongated spindle). (n) Number of cells analyzed. For details see legend to Fig. 2.

NUM1 fusion (FMY519) was grown to early log phase in YPD at 30°C. Nocodazole (Sigma-Aldrich) was added to 20 mg/ml and incubated for 1 h at 30°C. Cells were then incubated in YPGal with nocodazole (20 mg/ml) for 2 h at 30°C, fixed with formaldehyde, and stained for microtubules as above. Microscopy was carried out on an Axiophot microscope equipped with a 1.3 NA 100× Neofluar lens (Carl Zeiss, Inc.). Images were recorded using a SPOT camera (Visitron Systems GmbH) with a TWAIN driver. Adobe® Photoshop™ v5.0 and Canvas v3.5 were used to further optimize contrast.

Results

Cortical Num1p Dots at Mother/Daughter Poles May Serve as cMT Capture Sites during Late Anaphase

Num1p was previously localized in fixed cells by indirect immunofluorescence microscopy, using polyclonal antibodies against a COOH-terminal Num1p region (Farkasovsky and Küntzel, 1995). To study Num1p localization in living cells, we have introduced a PCR-generated cassette containing the *kanMX4* gene, the *GAL1* promoter, and a modified GFP gene (*yEGFP*) at the translational start of *NUM1* (Cormack et al., 1997). The diploid strain FMY519 (expressing the galactose-inducible GFP-Num1p fusion protein) was grown in 2% galactose (YPGal), and 0.3% glucose was added to reduce the extent of overexpression (Carminati and Stearns, 1997). Functionality of overproduced GFP-Num1p was tested by using the antibiotic polymyxin B, which is known to break bacterial membranes and to activate phospholipases (Boguslawski, 1992). We found *num1*Δ strains to be hypersensitive against polymyxin B during a chemotyping screen of several orphan gene deletants in the framework of the EUROFAN program (Rieger

Figure 2. (A and B) Subcellular distribution of GFP-Num1p in living diploid cells. (A) Strain FMY519 (relevant genotype *GAL1p-yEGFP3-NUM1/NUM1*) was grown in YPD to early exponential growth and induced in YPGal + 0.3% glucose for 2–3 h. (B, upper row) CEN.PK2 cells containing pFM313 (*NUM1p-yEGFP3-NUM1*, *CEN6/ARSH4*) were grown in YPD to early exponential phase. (B, lower row) CEN.PK2 cells containing the pRS416 derivatives pFM314 (a, GFP fused to Num1p residues 1–421), pFM315 (b, GFP fused to Num1p residues 1–1876) and the empty vector pRS416 (c). (C and D) Costaining of microtubules in FMY519 cells by indirect immunofluorescence using antitubulin antibodies. (D, upper row) Merged images of GFP-Num1p and microtubules; lower row, DAPI-stained nuclear regions.

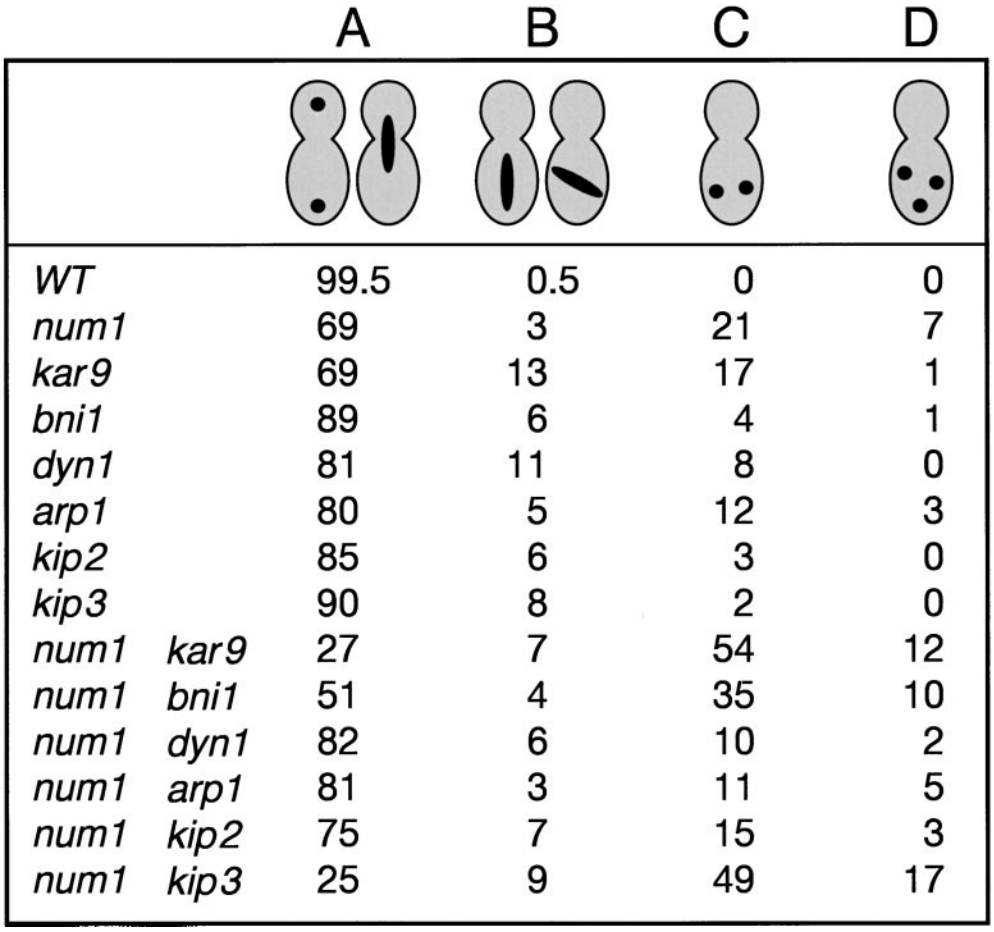

		A	B	C	D
WT		99.5	0.5	0	0
num1		69	3	21	7
kar9		69	13	17	1
bni1		89	6	4	1
dyn1		81	11	8	0
arp1		80	5	12	3
kip2		85	6	3	0
kip3		90	8	2	0
num1	*kar9*	27	7	54	12
num1	*bni1*	51	4	35	10
num1	*dyn1*	82	6	10	2
num1	*arp1*	81	3	11	5
num1	*kip2*	75	7	15	3
num1	*kip3*	25	9	49	17

Figure 5. Nuclear migration defects in null mutant cells. Haploid *MATa* cells were grown at 30°C to OD_{600} = 1.2 in YPD, fixed, and stained with DAPI, and 250–300 large-budded cells were scored for the position of nuclear regions. Strains: FMY691 (*WT*), FMY693 (*num1*Δ), FMY705 (*kar9*Δ), FMY711 (*bni1*Δ), FMY859 (*dyn1*Δ), FMY856 (*arp1*Δ), FMY848 (*kip2*Δ), FMY852 (*kip3*Δ), FMY799 (*num1*Δ *kar9*Δ), FMY821 (*num1*Δ *bni1*Δ), FMY789 (*num1*Δ *dyn1*Δ), FMY793 (*num1*Δ *arp1*Δ), FMY850 (*num1*Δ *kip2*Δ), and FMY854 (*num1*Δ *kip3*Δ). D includes cells with three or more nuclei in the mother compartment. >80% of the *num1*Δ *kar9*Δ, *num1*Δ *bni1*Δ, and *num1*Δ *kip3*Δ cells listed under D are multinucleate and multibudded.

et al., 1999). The reason why the *NUM1* deletion causes polymyxin B hypersensitivity is not known (see Discussion).

Fig. 1 indicates that the *NUM1* wild-type strain FMY691 grows well on YPGal containing 0.3 mg polymyxin B (row a), whereas the *num1*Δ strain FMY693 does not grow under these conditions (row c). Strain FMY627 expressing a galactose-inducible *yEGFP-NUM1* fusion gene grows like wild type (Fig. 1, row b), suggesting that the fusion protein is functional like Num1p in conferring polymyxin B resistance. Furthermore, a centromeric plasmid expressing *yEGFP-NUM1* under the control of the *NUM1* promoter (pFM313) rescues the nuclear migration defect of *num1*Δ strains (data not shown).

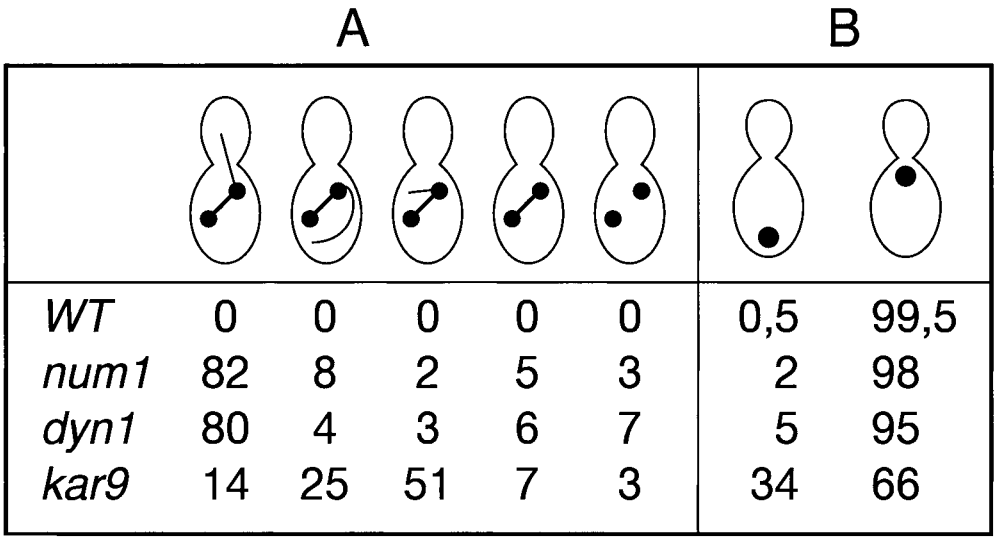

	A					B	
WT	0	0	0	0	0	0,5	99,5
num1	82	8	2	5	3	2	98
dyn1	80	4	3	6	7	5	95
kar9	14	25	51	7	3	34	66

Figure 6. (A) cMT orientation in *MATa* mutant cells containing two DAPI-stained chromosomal regions in the mother compartment. Strains FMY691 (*WT*), FMY705 (*kar9*Δ), FMY859 (*dyn1*Δ), and FMY693 (*num1*Δ) were grown to late exponential phase at 30°C and fixed for indirect immunofluorescence using antitubulin antibodies. 120–150 binucleate cells per mutant strain were scored for cMT orientation. (B) Nuclear position in preanaphase *MATa* wild-type and mutant cells. Strains: FMY691 (*WT*), FMY693 (*num1*Δ), FMY705 (*kar9*Δ), FMY859 (*dyn1*Δ), FMY799 (*num1*Δ *kar9*Δ), FMY789 (*num1*Δ *dyn1*Δ). Strains were grown to early exponential phase at 30°C, and 200–250 DAPI-stained preanaphase cells (single nucleus in the mother) were scored for each strain.

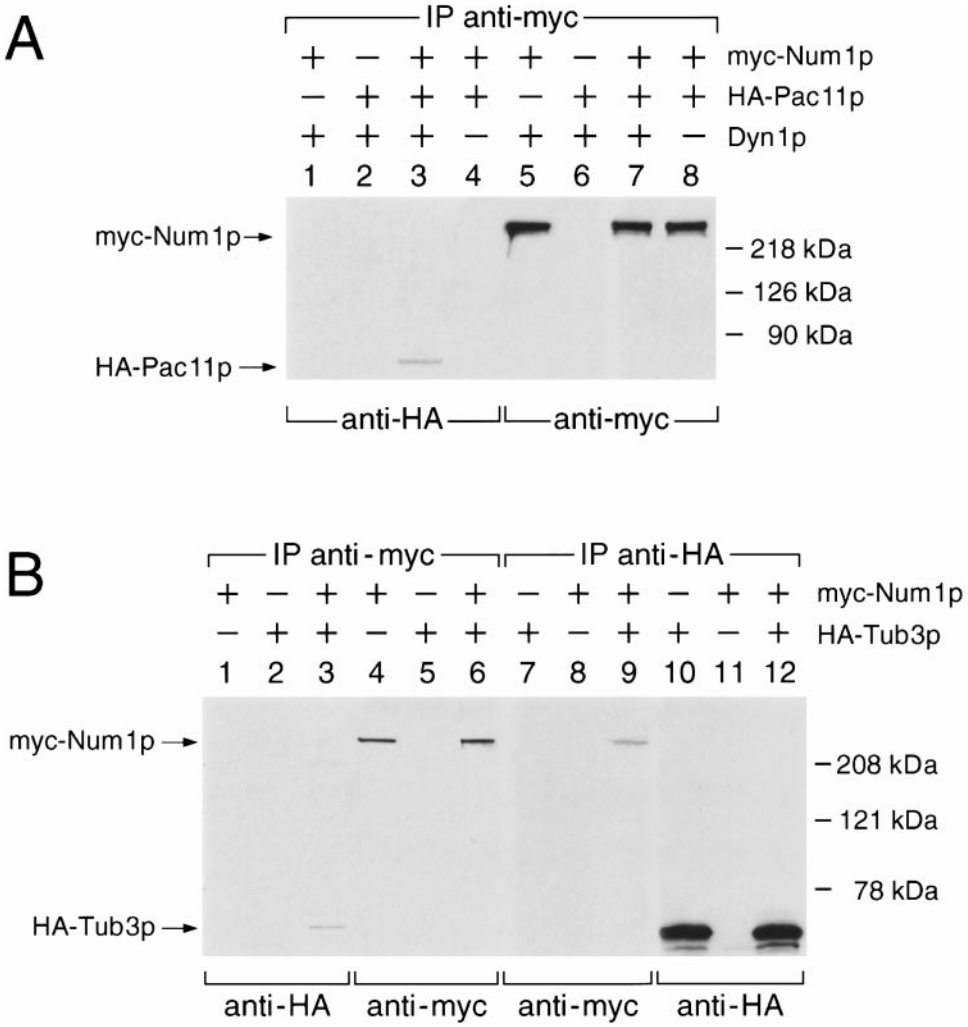

Figure 7. Coimmune precipitation of Myc-Num1p with HA-Pac11p (A) and HA-Tub3p (B). (A) Anti-Myc immunoprecipitates obtained from strains FMY684 (lanes 1 and 5), FMY899 (lanes 2 and 6), FMY905 (lanes 3 and 7), and FMY912 (lanes 4 and 8). (B) Anti-Myc immunoprecipitates obtained from strains FMY684 (lanes 1 and 4), FMY682 (lanes 2 and 5) and FMY603 (lanes 3 and 6) were probed with anti-HA (lanes 1–3) and anti-Myc (lanes 4–6) antibodies. Anti-HA immunoprecipitates obtained from strains FMY682 (lanes 7 and 10), FMY684 (lanes 8 and 11), and FMY603 (lanes 9 and 12) were probed with anti-Myc (lanes 7–9) and anti-HA (lanes 10–12) antibodies.

Fig. 2 A visualizes the cellular distribution of galactose-induced GFP-Num1p in living diploid cells. In addition to the previously noted dot-like Num1p distribution at the mother cortex, we observe prominent dots at the bud tip, the opposite pole of the mother compartment, and the bud neck, which were not visible in fixed *NUM1* cells treated with anti-Num1p antibodies (Farkasovsky and Küntzel, 1995). A similar distribution of GFP-Num1p was observed in galactose-grown haploid cells (data not shown). Furthermore, a *yEGFP3-NUM1* fusion gene was placed under the control of the *NUM1* promoter and introduced into the diploid wt strain CEN.PK2 as a centromeric plasmid (pFM313).

Fig. 2 B (upper row) shows the localization of GFP-Num1p as distinct dots at both poles of large-budded pFM313–containing cells. The exposure time of Fig. 2 B (GFP-Num1p controlled by the *NUM1* promoter) was increased fourfold compared with Fig. 2, A, C, and D (GFP-Num1p controlled by the *GAL1* promoter). Therefore, the intensities of the GFP signals do not reflect the level of expression. The lower row of Fig. 2 B shows large-budded cells expressing GFP-fusions to NH_2-terminal Num1p residues 1–421 (a) and 1–1876 (b) under the control of the *NUM1* promoter (pFM314 and pFM315, respectively). As previously noted, Num1p variants lacking the COOH-terminal PH domain are found in the cytoplasma and do not localize to the cell cortex (Farkasovsky and Küntzel, 1995).

We have stained microtubules with antitubulin antibodies in cells expressing galactose-induced GFP-Num1p in order to visualize possible cMT interactions with cortical Num1p dots. The cMTs of cells seen in Fig. 2, C and D, d, appear to intersect the Num1p dots at both cellular poles in late anaphase cells. A cell in a middle stage of anaphase is seen in Fig. 2 D, c: the Num1p dot at the bud tip appears to be in contact with cMTs, whereas mother-oriented cMTs seem to touch a lateral region of the mother cortex. A visual inspection of preanaphase cells (short spindle close to the bud neck; Fig. 2 D, a and b) revealed the presence of faintly stained cMTs orienting towards the bud tip.

Fig. 3 summarizes the appearance of prominent galactose-induced GFP-Num1p dots in cells of various cell cycle stages (less prominent dots at the mother cortex are not depicted). Two opposite Num1p dots are seen in 96% of G1 cells; one of the two dots is close to the incipient bud site and appears to persist at the mother side of the neck through S, G2, and M phase. The tip of the growing bud is marked by a Num1p dot at S/G2 and persists through mitosis.

The interactions of cMTs with galactose-induced cortical Num1p dots at the poles of anaphase cells (Fig. 2, C and D) are summarized in Fig. 4. A contact of cMTs to both polar Num1p dots is not observed in early anaphase cells, but is seen in 9% of mid anaphase and in 64% of late anaphase cells (Fig. 4, column A). cMTs appear to contact

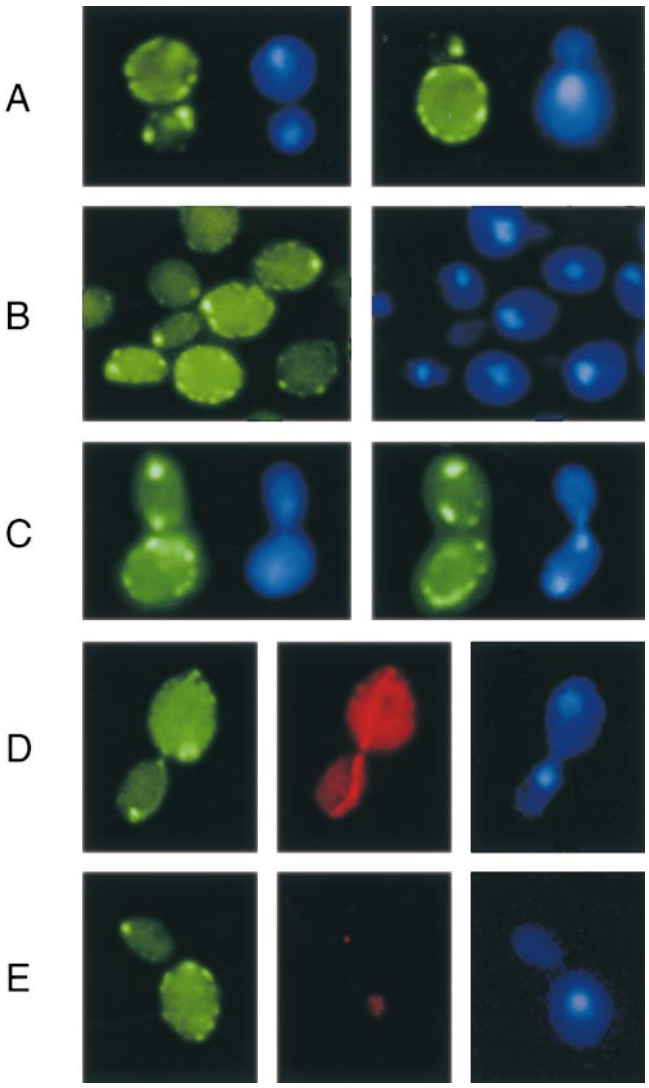

Figure 8. Subcellular distribution of GFP-Num1p in diploid strains lacking Bni1p (A, FMY795), Kar9p (B, FMY838), or Dyn1p (C, FMY872). (D and E) show diploid cells expressing galactose-induced *yEGFP3-NUM1* (FMY519) in the absence (D) or presence (E) of 20 μg/ml nocodazole. Microtubules were visualized by indirect immunofluorescence using antitubulin antibodies (middle panel of rows D and E), and nuclear regions were stained with DAPI (rows A–E, right).

Num1p at the bud tip but not at the opposite mother pole in 23% of early anaphase, 65% of mid anaphase, and 28% of late anaphase cells (Fig. 4, column B). cMTs contacting lateral regions of the bud and mother cortex, instead of touching the cellular poles, are seen in 72% of early anaphase, 26% of mid anaphase, and 8% of late anaphase cells (Fig. 4, column C).

We have also studied cMT contacts with polar Num1p dots in a diploid *dyn1*Δ/*dyn1*Δ strain expressing galactose-induced GFP-Num1p (FMY872). As summarized in Fig. 4, the percentage of late anaphase cells showing cMT contacts to both Num1p dots (A) is significantly reduced in the absence of Dyn1p (36% in *dyn1*Δ compared with 64% in wild type), whereas the percentage of cells with no cMT–Num1p contact (C) increases from 8% (wild type) to 42% (*dyn1*Δ). These observations suggest that the dynein heavy chain Dyn1p is involved in cMT capture at polar Num1p sites.

Num1p Acts in a Dynein–Dynactin–Kip2p-dependent Anaphase Pathway but Is Not Required for Kar9p-dependent Preanaphase Nuclear Positioning

The three double mutants *num1*Δ *kar9*Δ, *num1*Δ *bni1*Δ, and *num1*Δ *kip3*Δ exhibit additive defects in nuclear migration through the bud neck, as summarized in Fig. 5: the percentage of large-budded cells with more than one DAPI spot in the mother compartment ("binucleate mother cells") is increased in comparison to the single mutants. In contrast, the *num1*Δ combinations with *dyn1*Δ, *arp1*Δ, and *kip2*Δ are not significantly affected. Furthermore, the double mutants *num1*Δ *kar9*Δ and *num1*Δ *kip3*Δ grow slowly at 30°C and arrest at 15°C, whereas all other single and double mutants, including *num1*Δ *bni1*Δ, grow like wild type at both temperatures.

Fig. 6 A quantifies the distribution of binucleate mother cells with differing cMT morphologies in *num1*Δ, *dyn1*Δ, and *kar9*Δ strains, as revealed by indirect immunofluorescence of cells treated with antitubulin antibodies and DAPI. Approximately 80% of *num1*Δ and *dyn1*Δ cells of this nuclear phenotype contain long cMTs traversing the bud neck, as previously noted (Farkasovsky and Küntzel, 1995; Carminati and Stearns, 1997; Miller et al., 1998), whereas cMTs do not enter the bud in the majority of *kar9*Δ binucleate mother cells (Miller and Rose, 1998). It is interesting to note that *bni1*Δ mutants are much more related to *num1*Δ or *dyn1*Δ mutants than to *kar9*Δ or *bim1*Δ mutants according the cMT phenotype of binucleate mother cells: cMTs extend into the bud in 79–90% of binucleate *bni1*Δ cells (Fujiwara et al., 1999; Miller et al., 1999).

The data of Fig. 6 B demonstrate that nuclear migration to the bud neck in preanaphase cells does not require Num1p or Dyn1p, but partially depends on Kar9p. The double mutant *num1*Δ *dyn1*Δ (FMY789) corresponds phenotypically to the two single mutants (nuclear position close to the bud neck in 96% of preanaphase cells), whereas the *num1*Δ *kar9*Δ strain FMY799 exhibits a similar migration defect (only 62% of preanaphase cells with a nuclear position at the bud neck) as the *kar9*Δ single mutant.

The properties and genetic interactions of *num1*Δ mutants, as summarized in Figs. 5 and 6 and Table III, imply that Num1p acts in a Dyn1p–Arp1p–Kip2p pathway, but is not involved in a partially redundant Kar9p–Bim1p–Kip3p pathway.

Num1p Forms a Complex with the Dynein Intermediate Chain Pac11p and with the α-Tubulin Tub3p

The observed cMT capture by polar Num1p dots, the partial Dyn1p-dependency of these cMT–cortex interactions and the function of Num1p within a dynein pathway led us to test physical interactions of Num1p with the α-tubulin Tub3p and the dynein intermediate chain Pac11p by coimmune precipitation of epitope-tagged proteins. The nuclear migration defect of *pac11* mutants is similar to that of *num1*Δ and *dyn1*Δ strains, suggesting that the three proteins act in the same functional class (Geiser et al., 1997). We introduced the epitopes 3xMyc or 3xHA at the translational starts of *NUM1*, *PAC11*, and *TUB3* by inserting PCR-derived *kanM X4-GAL1p-3xMyc* or *kanMX4-*

Table III. Properties of Nuclear Migration Mutants

Mutant	cMTs extend into bud in most cells*	Cell stage affected	Reference
*kar9*Δ	No	Preanaphase	Miller et al., 1999
*bim1*Δ	No	Preanaphase	Adames and Cooper, 2000
*kip3*Δ	No	Preanaphase	Miller et al., 1998
*bni1*Δ	Yes	Preanaphase	Miller et al., 1999; Fujiwara et al., 1999
*num1*Δ	Yes	Anaphase	Farkasovsky and Küntzel, 1995; Geiser et al., 1997; this study
*dyn1*Δ	Yes	Anaphase	Miller et al., 1998; Carminati and Stearns, 1997
*kip2*Δ	Yes	Anaphase	Miller et al., 1998

*Binucleate mother cells (telophase in mother).

GAL1p-3xHA cassettes (Longtine et al., 1998). The functionality of the epitope-tagged proteins was demonstrated by an unimpaired nuclear migration phenotype of galactose-grown haploid strains expressing c-Myc (Myc)– or hemagglutinin (HA)-tagged proteins. In addition, haploid *num1::kanMX4-GAL1p-3xMyc-NUM1* strains showed the polymyxin B sensitivity of wild-type strains (Fig. 1), if grown in YPGal (data not shown). Western blot analysis of crude lysates of galactose-grown strains showed the expression of a 320-kD Myc-Num1p and a 60-kD HA-Pac11p protein (data not shown). Crude lysates of cells grown in galactose medium were treated with purified anti-Myc mAbs, and the immunocomplex was absorbed to protein A–conjugated Sepharose beads. The immunoprecipitate was then probed by Western blotting using anti-HA or anti-Myc antibodies.

Fig. 7 A demonstrates that HA-Pac11p coprecipitates with Myc-Num1p in a wild-type background (lane 3, strain FMY905) but not in the absence of Dyn1p (lane 4, strain FMY912). Furthermore, the 60-kD HA-Pac11p band is absent from anti-Myc precipitates of cells expressing only HA-Pac11p (lane 2, strain FMY899), supporting the specificity of the coprecipitation. Lanes 5 to 8 of Fig. 7 A confirm the presence or absence of Myc-Num1p in the anti-Myc precipitates. Similarly, the results shown in Fig. 7 B indicate that HA-Tub3p (50 kD) coprecipitates with Myc-Num1p (Fig. 7, lane 3), and Myc-Num1p coprecipitates with HA-Tub3p (Fig. 7, lane 9). The specificity of these coprecipitations is documented in Fig. 7, lanes 2 and 8.

Num1p Associates with Bni1p–Kar9p at the Bud Tip of Early Anaphase Cells

Num1p may transiently coexist or even cooperate with a Bni1p–Kar9p complex at the bud tip, although the two cor-

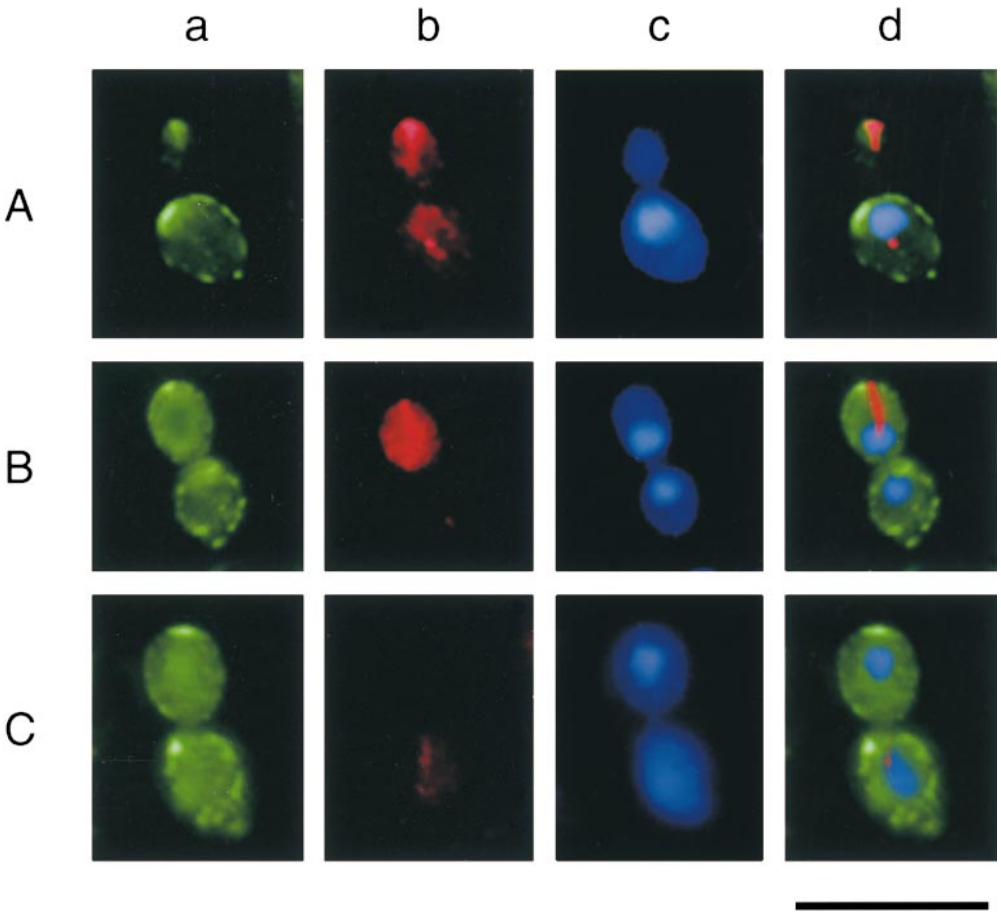

Figure 9. Covisualization of GFP-Num1p, 3xHA-Kar9p, and chromosomal DNA in (A) pre-anaphase, (B) mid anaphase, and (C) late anaphase/telophase cells. Strain FMY861 was grown in YPGal + 0.3% glucose at 30°C for 3 h. Formaldehyde-fixed cells were treated with anti-HA mAb and visualized by indirect immunofluorescence. Bar, 10 μm.

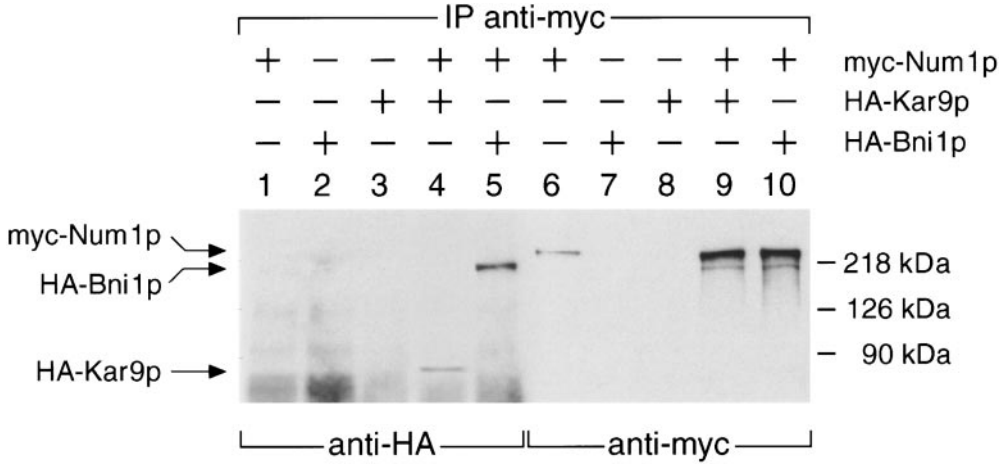

Figure 10. Coimmune precipitation of 3xMyc-Num1p with 3xHA-Bni1p and 3xHA-Kar9p. Anti-Myc immunoprecipitates obtained from strains FMY684 (lanes 1 and 6), FMY78 (lanes 2 and 7), FMY810 (lanes 3 and 8), FMY809 (lanes 4 and 9), and FMY805 (lanes 5 and 10) were probed with anti-HA (lanes 1–5) and anti-Myc (lanes 6–10) antibodies.

tical cMT capture sites appear to operate at different stages of the cell cycle (see Discussion). To test this possibility, we have studied the influence of Bni1p, Kar9p, and Dyn1p on the bud tip localization of GFP-Num1p. The two Bni1p-deficient diploid cells (FMY795) shown in Fig. 8 A contain a prominent GFP-Num1p dot at a lateral region of the bud cortex, in addition to several dots at the mother cortex, whereas a Num1p dot at the bud tip is clearly missing in virtually all observed budded cells. In contrast, a prominent GFP-Num1p dot is seen at the bud tip of cells lacking either Kar9p (Fig. 8 B) or Dyn1p (Fig. 8 C).

We have also addressed the question whether cMTs influence the Num1p deposition at the bud tip by treating cells with nocodazole before galactose induction of GFP-Num1p: 31% of nocodazole-treated large-budded cells lacked microtubules but contained the bud tip dot of GFP-Num1p, as shown in Fig. 8 E, whereas the bud tip dot of GFP-Num1p was observed in 28% of mock-treated (DMSO) large-budded cells (Fig. 8 D), suggesting that cMTs are not required for targeting Num1p to the bud tip cortex.

Fig. 9 depicts cells of a diploid strain (FMY861) coexpressing galactose-inducible *yEGFP3-NUM1* and *3xHA-KAR9* fusion genes. Cells were grown in YPGal to early exponential phase and treated with anti-HA mAbs after fixation. DAPI was added to the mounting medium to stain chromosomal regions. Fig. 9, row A, shows a preanaphase cell containing a HA-Kar9p patch at the bud tip (lanes b and d), which apparently represents a cortical cMT/Kar9p capture site visualizing the plus-end of cMTs by microtubule-bound Kar9p (Miller et al., 1999). The same cell contains a GFP-Num1p patch at the bud tip, which is only partially resolved from the HA-Kar9p patch, as seen in the merged image of Fig. 9, lane d. Fig. 9, row B, shows a cell at early anaphase stage with a GFP-Num1p dot (lane a) and a cMT/HA-Kar9p capture site (lane b) at the bud tip. The merged image of Fig. 9, lane d, clearly resolves the two apparently adjacent cortical GFP-Num1p and HA-Kar9p dots and further demonstrates that the Kar9p-decorated cMTs are in contact with cortical HA-Kar9p but not with GFP-Num1p. HA-Kar9p and GFP-Num1p contact or near proximity was observed in 29% of early anaphase and 75% of mid anaphase cells with Kar9p localization at the bud cortex (dot or line). Anti–HA-stained HA-Kar9p has completely disappeared from the bud at the late anaphase/telophase stage (>90%), as seen in Fig. 9, row C, lane b, whereas GFP-Num1p persists at the bud tip (Fig. 9, lanes a and b).

The close neighborhood of Num1p and Kar9p dots at the bud tip of early anaphase cells may indicate a transient physical association of Num1p with Kar9p-binding Bni1p at the bud tip cortex. Indeed, we observe a coimmunoprecipitation of Myc-Num1p with HA-Bni1p and HA-Kar9p, as shown in Fig. 10, lanes 4 and 5, respectively. Anti-Myc precipitates of cells expressing only HA-Bni1p (FMY783) or HA-Kar9p (FMY810) do not contain the 219-kD HA-Bni1p band (Fig. 10, lane 2) or the 74 kD HA-Kar9p band (Fig. 10, lane 3), supporting the specificity of the coprecipitation. The presence of Myc-Num1p in the anti-Myc precipitates was confirmed by anti-Myc probing (Fig. 10, lanes 6, 9, and 10).

Discussion

The data presented in this study suggest that Num1p controls the dynein-dependent migration of the elongating nuclear spindle through the bud neck by forming a cortical cMT capture site at the bud tip; a second Num1p/cMT capture site at the opposite mother pole appears to be involved in late anaphase/telophase cells. We further suggest that cortical capture and pulling of cMTs at the Num1p sites is mediated by the dynein intermediate chain Pac11p. Our conclusions and suggestions are based on the following observations: (a) Genetic and phenotypic analyses of *num1*Δ strains indicate that Num1p is not required for Bni1p–Kar9p–Bim1p–Kip3p-dependent nuclear migration to the bud neck in preanaphase cells but acts within a dynein–dynactin–Kip2p pathway, controlling nuclear migration through the bud neck and spindle elongation in anaphase cells; (b) GFP-Num1p localizes at the bud tip and the opposite pole of the mother cortex in living cells, and cMTs appear to intersect the Num1p dot at the bud tip during mid anaphase and to touch both polar Num1p dots at late anaphase/telophase; and (c) Num1p forms a complex with the dynein intermediate chain Pac11p and with the α-tubulin Tub3p, as shown by coimmune precipitation of Myc- or HA-tagged proteins. Pac11p has previously been shown to coprecipitate with the dynein heavy chain Dyn1p (Kahana et al., 1998) and to act together with Num1p (= Pac12p) in a cytoplasmic dynein pathway (Geiser et al., 1997). Furthermore, our data indicate that the Num1p–Pac11p interaction as well as the Num1p–cMT contacts depends on the presence of Dyn1p, suggesting that Num1p serves to attach the Dyn1p motor domain and the plus-end of cMTs to the cellular cortex.

Another component of the yeast dynein pathway is the 54-kD Pac1 protein (Geiser et al., 1997), a homologue of the *Aspergillus nidulans* NudF protein (Xiang et al., 1995) and the human lissencephaly protein Lis1 (Reiner et al., 1993). Mammalian Lis1p is required for microtubule organization and the regulation of cytoplasmic dynein during neuronal proliferation, migration, and morphogenesis (Faulkner et al., 2000; Smith et al., 2000). The *Drosophila* homologue DLis1 acts as a cortical anchor for the dynein–dynactin complex during nuclear positioning in oocytes (Swan et al., 1999). Although Pac1p has not yet been localized in yeast cells, it may participate in cortical cMT capture by interacting with Num1p and/or Dyn1p.

Num1p contains a COOH-terminal PH domain that is essential for cortical association and nuclear migration functions (Farkasovsky and Küntzel, 1995). PH domains of several proteins are known to interact with the lipid phosphatidylinositol 4,5-bisphosphate (PIP_2) (Lemmon et al., 1996), and Num1p may bind to the inner face of the plasma membrane via its PH domain. We have shown that the Num1p PH domain is sufficient to target GST (glutathione *S*-transferase) to the cortex of yeast cells; furthermore, Num1p physically interacts with PIP_2-specific phospholipase C, as revealed by two-hybrid and coimmune precipitation experiments (Martin, 1998; our unpublished data).

The postulated membrane interaction of Num1p may possibly be involved in protecting yeast cells against the membrane-breaking antibiotic polymyxin B (Boguslawski, 1992), resulting in the observed hypersensitivity of *num1*Δ strains.

Two observations suggest that Num1p interacts with the formin Bni1p, another cortical protein forming a cMT capture site at the bud tip (Heil-Chapdelaine et al., 2000; Lee et al., 1999; Korinek et al., 2000; Lee et al., 2000): Myc-Num1p coprecipitates with HA-Bni1p, and the GFP-Num1p dot at the bud cortex is shifted to a lateral region in the absence of Bni1p. Costaining experiments have revealed that the Bni1p-binding protein Kar9p localizes at the bud tip of early and mid anaphase cells at a region adjacent to, but not superimposing with, the Num1p dot. Furthermore, bud-oriented cMTs appear to intersect a cortical Kar9p capture site, without being in contact with the adjacent Num1p dot at the bud tip (Miller and Rose, 1998; Lee et al., 2000; this study, Fig. 9 B).

Thus, the two types of cortical cMT capture sites (Bni1p–Kar9p and Num1p–Pac11p) seem to be in close proximity or even in physical contact at least during early and middle anaphase, although they control two temporally separated steps of nuclear migration. Our observation that the GFP-Num1p localization depends on Bni1p but not on Kar9p (Fig. 8) suggests an indirect Num1p–Kar9p interaction via Bni1p; indeed, a two-hybrid assay failed to reveal physical interactions between Num1p and Kar9p peptides (data not shown).

A cell cycle–specific transient interaction between the two cortical complexes Bni1p–Kar9p and Num1p–dynein may help to control the transition from Kar9p- to dynein-dependent nuclear migration: Kar9p disappears from the bud cortex at late anaphase/telophase (Miller and Rose, 1998), whereas Num1p remains at the bud tip and the opposite pole of the mother cell. This final stage of mitosis may require both Num1p sites to draw the two spindle pole bodies (SPBs) close to the cellular poles, and both Num1p/cMT capture sites may bind the minus-end–directed dynein motor via its subunit Pac11p. It is interesting to note that the dynein-activating dynactin subunit Nip100p localizes to the SPBs throughout the cell cycle, but is never seen at the cell cortex; furthermore, the dynactin subunits Nip100p, Arp1p, and Jnm1p form a 15.5S complex that does not include the dynein subunits Dyn1p and Pac11p (Kahana et al., 1998). These observations would predict that the SPB-bound dynactin complex can transiently interact with the cortically associated dynein complex only after pulling the SPBs close to the cellular poles. The cortex–SPB contact may then trigger signals for spindle collapse, nuclear reorganization, and cytokinesis.

The authors wish to thank Oliver Stiedel for help with digital imaging, and Ludwig Kolb for technical assistance.

References

Adames, N.R., and J.A. Cooper. 2000. Microtubule interactions with the cell cortex causing nuclear movements in *Saccharomyces cerevisiae*. *J. Cell Biol.* 149:863–874.

Ansari, K., S. Martin, M. Farkasovsky, I.-M. Ehbrecht, and H. Küntzel. 1999. Phospholipase C binds to the receptor-like Gpr1 protein and controls pseudohyphal differentiation in *Saccharomyces cerevisiae*. *J. Biol. Chem.* 274:30052–30058.

Ausubel, F.M., R.E. Kingston, R. Brent, D.D. Moore, J.G. Seidman, J.A. Smith, and K. Struhl. 1993. Current Protocols in Molecular Biology. Vol. 2. Greene Publishing Associates and Wiley Interscience, New York. 13.a1–13.3.12.

Boguslawski, G. 1992. *PBS2*, a yeast gene encoding a putative protein kinase, interacts with the *RAS2* pathway and affects osmotic sensitivity of *Saccharomyces cerevisiae*. *J. Gen. Microbiol.* 138:2425–2432.

Carminati, J.L., and T. Stearns. 1997. Microtubules orient the mitotic spindle in yeast through dynein-dependent interactions with the cell cortex. *J. Cell Biol.* 138:629–641.

Cormack, B.P., G. Bertram, M. Egerton, N.A.R. Gow, S. Falkow, and A.J.P. Brown. 1997. Yeast-enhanced green fluorescent protein (yEGFP): a reporter of gene expression in *Candida albicans*. *Microbiology.* 143:303–311.

Cottingham, F.R., and M.A. Hoyt. 1997. Mitotic spindle positioning in *Saccharomyces cerevisiae* is accomplished by antagonistically acting microtubule motor proteins. *J. Cell Biol.* 138:1041–1053.

DeZwaan, T.M., E. Ellingson, D. Pellman, and D.M. Roof. 1997. Kinesin-related *KIP3* of *Saccharomyces cerevisiae* is required for a distinct step in nuclear migration. *J. Cell Biol.* 138:1023–1040.

Farkasovsky, M., and H. Küntzel. 1995. Yeast Num1p associates with the mother cell cortex during S/G2 phase and affects microtubular functions. *J. Cell Biol.* 131:1003–1014.

Faulkner, N.E., D.L. Dujardin, C.-Y. Tai, K.T. Vaughan, C.B. O'Connell, Y. Wang, and R.B. Vallee. 2000. A role for the lissencephaly gene LIS1 in mitosis and cytoplasmic dynein function. *Nat. Cell Biol.* 2:784–791.

Fujiwara, T., K. Tanaka, E. Inoue, M. Kikyo, and Y. Takai. 1999. Bni1p regulates microtubule-dependent nuclear migration through the actin cytoskeleton in *Saccharomyces cerevisiae*. *Mol. Cell. Biol.* 19:8016–8027.

Geiser, J.R., E.J. Schott, T.J. Kingsbury, N.B. Cole, L.J. Totis, G. Bhattacharyya, L. He, and M.A. Hoyt. 1997. *Saccharomyces cerevisiae* genes required in the absence of the *CIN8*-encoded spindle motor act in functionally diverse mitotic pathways. *Mol. Biol. Cell.* 8:1035–1050.

Güldener, U., S. Heck, T. Fiedler, J. Beinhauer, and J. Hegemann. 1996. A new efficient gene disruption cassette for repeated use in budding yeast. *Nucl. Acids Res.* 24:2519–2524.

Heald, R., and C.E. Walczak. 1999. Microtubule-based motor function in mitosis. *Curr. Opin. Struct. Biol.* 9:268–274.

Heil-Chapdelaine, R.A., N.K. Tran, and J.A. Cooper. 2000. Dynein-dependent movements of the mitotic spindle in *Saccharomyces cerevisiae* do not require filamentous actin. *Mol. Biol. Cell.* 11:863–872.

Hildebrandt, E.R., and M.A. Hoyt. 2000. Mitotic motors in *Saccharomyces cerevisiae*. *Biochim. Biophys. Acta.* 1496:99–116.

Kahana, J.A., G. Schlenstedt, D.M. Evanchuk, J.R. Geiser, M.A. Hoyt, and P.A. Silver. 1998. The yeast dynactin complex is involved in partitioning the mitotic spindle between mother and daughter cells during anaphase B. *Mol. Biol. Cell.* 9:1741–1756.

Karki, S., and E.L.F. Holzbaur. 1999. Cytoplasmic dynein and dynactin in cell division and intracellular transport. *Curr. Opin. Cell Biol.* 11:45–53.

Korinek, W.S., M.J. Copeland, A. Chaudhuri, and J. Chant. 2000. Molecular linkage underlying microtubule orientation toward cortical site in yeast. *Science.* 287:2257–2259.

Kormanec, J., I. Schaaff-Gerstenschläger, F.K. Zimmermann, D. Perecko, and H. Küntzel. 1991. Nuclear migration in *Saccharomyces cerevisiae* is controlled by the highly repetitive 313kDa NUM1 protein. *Mol. Gen. Genet.* 230:277–278.

Lee, L., S.K. Klee, M. Evangelista, C. Boone, and D. Pellman. 1999. Control of

mitotic spindle position by the *Saccharomyces cerevisiae* formin Bni1p. *J. Cell Biol.* 144:947–961.
Lee, L., J.S. Tirnauer, J. Li, S.C. Schuyler, J.Y. Liu, and D. Pellman. 2000. Positioning of the mitotic spindle by a cortical-microtubule capture mechanism. *Science.* 287:2260–2262.
Lemmon, M.A., K.M. Ferguson, and J. Schlessinger. 1996. PH domains: diverse sequences with a common fold recruit signaling molecules to the cell surface. *Cell.* 85:621–624.
Longtine, M.S., A. McKenzie III, D.J. Demarini, N.G. Shah, A. Wach, A. Brachat, P. Philippsen, and J.R. Pringle. 1998. Additional modules for versatile and economical PCR-based gene deletion and modification in *Saccharomyces cerevisiae. Yeast.* 14:953–961.
Martin, S. 1998. Genetic and physical interactions of the nuclear migration protein Num1p with phospholipase C (Plc1p) in *Saccharomyces cerevisiae*. Ph.D. thesis. University of Göttingen, Göttingen, Germany. 97 pp.
Miller, R.K., and M.D. Rose. 1998. Kar9p Is a novel cortical protein required for cytoplasmic microtubule orientation in yeast. *J. Cell Biol.* 140:377–390.
Miller, R.K., K.K. Heller, L. Frisèn, D.L. Wallack, D. Loayza, A.E. Gammie, and M.D. Rose. 1998. The kinesin-related proteins, Kip2p and Kip3p, function differently in nuclear migration in yeast. *Mol. Biol. Cell.* 9:2051–2068.
Miller, R.K., D. Matheos, and M.D. Rose. 1999. The cortical localization of the microtubule orientation protein, Kar9p, is dependent upon actin and proteins required for polarization. *J. Cell Biol.* 144:963–975.
Miller, R.K., S.-C. Cheng, and M.D. Rose. 2000. Bim1p/Yeb1p mediates the Kar9p-dependent cortical attachment of cytoplasmic microtubules. *Mol. Biol. Cell.* 11:2949–2959.
Muhua, L., T.S. Karpova, and J.A. Cooper. 1994. A yeast actin-related protein homologous to that in vertebrate dynactin complex is important for spindle orientation and nuclear migration. *Cell.* 78:669–679.
Reiner, O., R. Carrozzo, Y. Shen, M. Wehnert, F. Faustinella, W.B. Dobyns, C.T. Caskey, and D.H. Ledbetter. 1993. Isolation of a Miller-Dieker lissencephaly gene containing G protein beta-subunit-like repeats. *Nature.* 364: 717–721.
Revardel, E., and M. Aigle. 1993. The *NUM1* yeast gene: length polymorphism and physiological aspects of mutant phenotype. *Yeast.* 9:495–506.
Rieger, K.-J., M. El-Alama, G. Stein, C. Bradshaw, P.P. Slonimski, and K. Maundrell. 1999. Chemotyping of yeast mutants using robotics. *Yeast.* 15: 973–986.
Saunders, W.S., D. Koshland, D. Eshel, I.R. Gibbons, and M.A. Hoyt. 1995. *Saccharomyces cerevisiae* kinesin– and dynein–related proteins required for anaphase chromosome segregation. *J. Cell Biol.* 128:617–624.
Schwartz, K., K. Richards, and D. Botstein. 1997. *BIM1* encodes a microtubule-binding protein in yeast. *Mol. Biol. Cell.* 8:2677–2691.
Shaw, S.L., E. Yeh, P. Maddox, E.D. Salmon, and K. Bloom. 1997. Astral microtubule dynamics in yeast: a microtubule-based searching mechanism for spindle orientation and nuclear migration into the bud. *J. Cell Biol.* 139:985–994.
Shaw, S.L., P. Maddox, R.V. Skibbens, E. Yeh, E.D. Salmon, and K. Bloom. 1998. Nuclear and spindle dynamics in budding yeast. *Mol. Biol. Cell.* 9:1627–1631.
Smith, D.S., M. Niethammer, R. Ayala, Y. Zhou, M.J. Gambello, A. Wynshaw-Boris, and L.-H. Tsai. 2000. Regulation of cytoplasmic dynein behaviour and microtubule organization by mammalian Lis1. *Nat. Cell Biol.* 2:767–775.
Swan, A., T. Nguyen, and B. Suter. 1999. *Drosophila Lissencephaly-1* functions with *Bic-D* and dynein in oocyte determination and nuclear positioning. *Nature Cell Biol.* 1:444–449.
Theesfeld, C.L., J.E. Irazoqui, K. Bloom, and D.J. Lew. 1999. The role of actin in spindle orientation changes during the *Saccharomyces cerevisiae* cell cycle. *J. Cell Biol.* 146:1019–1031.
Tirnauer, J.S., E. O'Toole, L. Berrueta, B.E. Bierer, and D. Pellman. 1999. Yeast Bim1p promotes the G1-specific dynamics of microtubules. *J. Cell Biol.* 145:993–1007.
Xiang, X., A.H. Osmani, S.A. Osmani, M. Xin, and N.R. Morris. 1995. NudF, a nuclear migration gene in *Aspergillus nidulans*, is similar to the human *LIS-1* gene required for neural migration. *Mol. Biol. Cell.* 6:297–310.
Yeh, E., R.V. Skibbens, J.W. Cheng, E.D. Salmon, and K. Bloom. 1995. Spindle dynamics and cell cycle regulation of dynein in the budding yeast, *Saccharomyces cerevisiae. J. Cell Biol.* 130:687–700.